Received: 2 April 2021 | Revised: 14 January 2022 | Accepted: 29 January 2022

DOI: 10.1111/ter.12585

RESEARCH ARTICLE

Terra Nova WILEY

Pre-eruption magma staging at the long-lived intraplate Dunedin Volcano, New Zealand

Rachael J. M. Baxter[1,2] | James D. L. White[2] | Marco Brenna[2] | Christian Ohneiser[2]

[1]Department of Earth Sciences, Cambridge University, Cambridge, UK

[2]Geology Department, Otago University, Dunedin, New Zealand

Correspondence
Rachael J. M. Baxter, Department of Earth Sciences, Cambridge University, Downing Street, Cambridge CB2 3EQ, UK.
Email: rjmb3@cam.ac.uk

Funding information
NZ Federation of Graduate Women; University of Otago

Abstract

The oldest-known rocks of the eroded Dunedin Volcano (DV), New Zealand, active 16.0–11.0 Ma, were emplaced by penecontemporaneous explosive eruptions and intrusions of magmas with a remarkable range of compositions, including basanite, alkali basalt, trachyte and phonolite. The compositional diversity of magmas emplaced in rapid succession during the earliest development of the volcano signify the existence of a complex magmatic system and highly evolved magmas, typical of those attributed to mature magmatic systems; here it developed in concert with the volcano's surface eruptions. We infer that multiple deep and shallow reservoirs were suddenly tapped as volcanism commenced. DV repeatedly erupted the same range of magmas over 5 Myr, suggests that these distributed reservoirs failed to significantly integrate through millions of years of slow volcano growth.

1 | INTRODUCTION

Early histories of some small volcanoes have been established (Brenna et al., 2012; Németh et al., 2003) but investigations of the early development of large volcanoes are typically hindered by the burial of early products. Current understanding of a volcano's lifecycle are encapsulated in two, conflicting, generalizations: (1) Volcanoes begin erupting primitive compositions, producing evolved rocks over time with system evolution (Khalaf et al., 2018; Sato et al., 1990); (2) Volcanoes commence with evolved lavas, and primitive compositions erupt later after a stable conduit is established (Pánisová et al., 2018; Panter et al., 1997).

Volcanism, even that producing small (≤9 km^3; Wood, 1979) centres in single eruptions, has complexities, with bimodal compositions at monogenetic centres inferred to reflect 'failed eruptions' of early batches of magma injected into different levels of the lithosphere without erupting (Jankovics et al., 2015; Németh et al., 2003). Instead, they differentiated before being mobilized by mafic recharge that instigated ascent and eruption of the stored, more-buoyant fractionated melt; the mobilizing mafic magma followed closely behind. Similar compositional variation and system behaviour have been identified in other continental volcanic fields (Chevrel et al., 2016; Duda & Schmincke, 1985), and in historic eruptions of 'satellite' cones of ocean island volcanoes (e.g. Klügel et al., 2000).

Various continental volcanic fields (e.g. Eifel Volcanic Field, Germany; Trans-Mexican Volcanic Belt, Mexico; Klyuchevskoy Volcanic Group, Russia; Connor et al., 2000; Jeju Island, South Korea; Brenna et al., 2012) began with dispersed small volcanoes, amidst which complex, evolved centres with mature magma plumbing systems were later established. In intraplate settings, these produced a compositionally wide range of magmas above sites of peak mantle productivity (Brenna et al., 2012; Schmincke, 2007).

It remains unclear how these larger, more-complex volcanoes are born within regions of dispersed volcanism. Here, we analyse a small area that includes the oldest-dated rocks of the Dunedin Volcano

(DV), which resides among rocks of the Dunedin volcanic group (DVG; New Zealand) produced by small volcanoes dispersed over ~8,000 km^2 (e.g. Coombs et al., 2008; Scott et al., 2020). The compositional range and geometrical complexity of these early eruptive products, and their similarities with later ones, provide new information about how long-lived, low-output composite volcanoes originate and develop through their lives.

1.1 | The DV

The Miocene DV (Coombs et al., 2008) on the SE coast of New Zealand (Figure 1a) is one of many intraplate volcanoes of Zealandia (e.g. Hoernle et al., 2006), within the wider Cenozoic SW Pacific diffuse alkaline magmatic province (DAMP; Finn et al., 2005). The DV erupted basalt to phonolite, sporadically, over 5 Myr (16.0–11.0 Ma; Scott et al., 2020). Early submarine activity was explosive (Martin & White, 2001), with later subaerial effusive and explosive activity constructing a 25 km diameter edifice (Benson, 1968; Coombs et al., 2008). Peripheral lavas extend ~20 km north of the edifice centre (McLeod & White, 2018). The total erupted volume is poorly known, though Coombs et al. (1986) inferred that 150 km^3 of material is represented by the volcano, while gravity modelling indicates 600 km^3 of magma was captured in the crust (Reilly, 1972).

The oldest-known rocks of the DV are exposed at Otapahi (Allans Beach; Figure 1b). Shallow submarine pyroclastic deposits (Martin & White, 2001, 2002) are cross-cut by dikes, one of which yielded the oldest Ar^{39}/Ar^{40} date of 16.0 ± 0.4 Ma (Hoernle et al., 2006). About half a km of Cenozoic sedimentary rocks underlie the DV above a Mesozoic schist basement.

2 | METHODS

Fieldwork established relative age relationships between dikes, and host volcaniclastic units, and to collect samples for petrographic, whole-rock and EMPA analyses, as well as magnetic polarity experiments (full methodologies in File S1).

3 | RESULTS

A phonolite pumice unit (Martin & White, 2002) that is crystal-poor at the base, transitioning to crystal-rich near the top with phenocrysts of olivine, plagioclase, clinopyroxene and amphibole, hosts an abundance of cross-cutting diatremes and dikes (e.g. Figures S1 and S2; Baxter & White, submitted). Other than PLb lapillistone, older diatremes contain no igneous lithic clasts, strongly suggesting no volcanism occurred at Otapahi prior to formation of the Pumice Lapilli-beds (PLb). Peperites occur where dikes cut both the PLb (Figure 1b,c,d), and diatreme deposits.

Compositionally and texturally diverse dikes are extensively mingled together, forming dike complexes (Figure 1c–e; Figures S3–S5). Mineral assemblages, modal mineral compositions, and trace element concentrations reveal compositional diversity of dikes mingled together (Figures 1d and 2; File S3). Although composition classifications range from alkaline basalt to trachyte (Figure 2a) alteration obscures the true compositional range and abundance of emplacement events at Otapahi (Table 1). The range of immobile element ratios for dikes from Otapahi exceed the vast majority of Zr/Ti ratios reported for volcanic rocks from DV (Figure 2b). Trace elements demonstrate the range of compositional variability not encapsulated within rock classification by a TAS diagram (Figure 2c; Table 1). Among alkali basalt samples, one is enriched in alkalis and incompatible trace elements compared to others sampled. Similar enrichment differences appear among trachytes sampled.

Petrographic textures and mineral modal abundances and assemblages support additional variation of dikes not captured by whole-rock compositions (Figures 1e and 2d). Modal abundances indicate the presence of a basanite dike at Otapahi, not represented by whole-rock major elements, as well as suggest the presence of altered phonolites (Figure 2d). Although major elements indicate the most evolved rocks in the area to be trachytes, immobile trace element abundances and modal minerologies indicate some trachytes

Statement of significance

Do compositionally complex volcanoes grow from simple beginnings, or does their complexity manifest at a very early age? The Dunedin Volcano (New Zealand) is the surface expression of a long-lived (16–11 Ma) intraplate magmatic system. Magma of a remarkably wide compositional range was over a short time interval injected through and mingled with some of the earliest volcanic deposits, indicating that a mature and complex magma plumbing system had already developed as the embryonic volcano began to grow.

FIGURE 1 (a) Dunedin Volcano on the SE coast of NZ erupted diverse alkaline lavas across 5 Myr. Red stars indicate pre-volcanic rock exposed the closest to Otapahi (b) aerial image and superimposed photogrammetry of Otapahi, Otago peninsula. Enlargement (c) of headland with volcaniclastic units cut by compositionally diverse dikes mingled together or forming peperites. (d) Photo (I) and annotation (II) of cliffside with multiple dikes (*D*); dikes mingled within pumice lapilli beds (PLb) forming peperite. (III) porphyritic alkali basalt (Alk a) intrudes PLb with peperite (P) contact. (IV) mingling of Alk a with enriched alkali basalt, Alk B. (V) Mingled alkali basalts, cross-cut by sinuous trachybasalt (Trb). Hammer~40 cm. (e) Petrographic sections from four dikes mingled, Alk a (I), Alk B (II), tr (III) and Bta (IV) shown in 2C. LHS, cross-polarized light; RHS, plane-polarized light

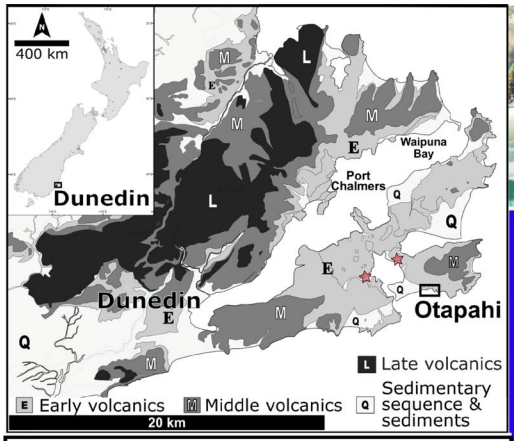
400 km
Dunedin
Waipuna Bay
Port Chalmers
Dunedin
Otapahi
L Late volcanics
E Early volcanics
M Middle volcanics
Q Sedimentary sequence & sediments
20 km


(b)

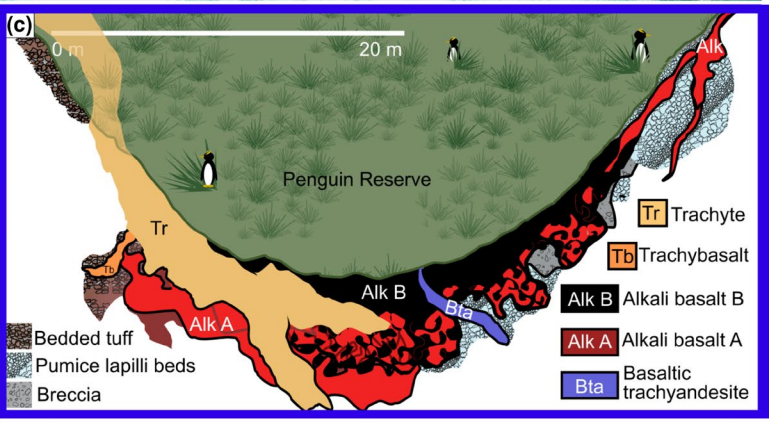
(c)
0 m
20 m
Alk
Penguin Reserve
Tr
Th
Alk B
Bta
Alk A
Bedded tuff
Pumice lapilli beds
Breccia
Tr Trachyte
Tb Trachybasalt
Alk B Alkali basalt B
Alk A Alkali basalt A
Bta Basaltic trachyandesite

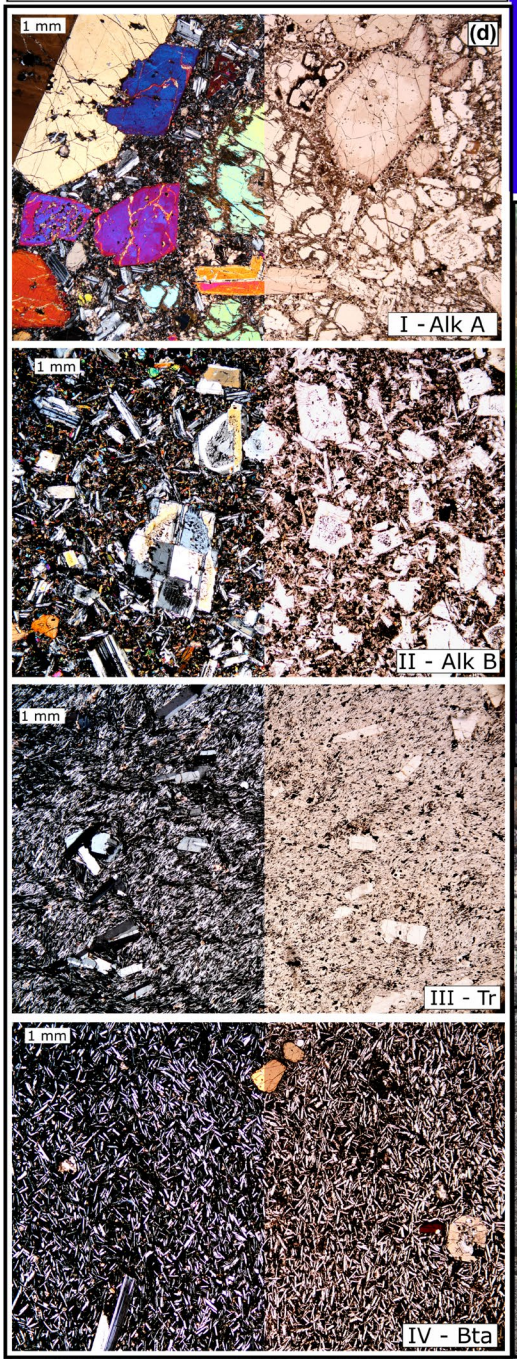
1 mm
(d)
I - Alk A
1 mm
II - Alk B
1 mm
III - Tr
1 mm
IV - Bta

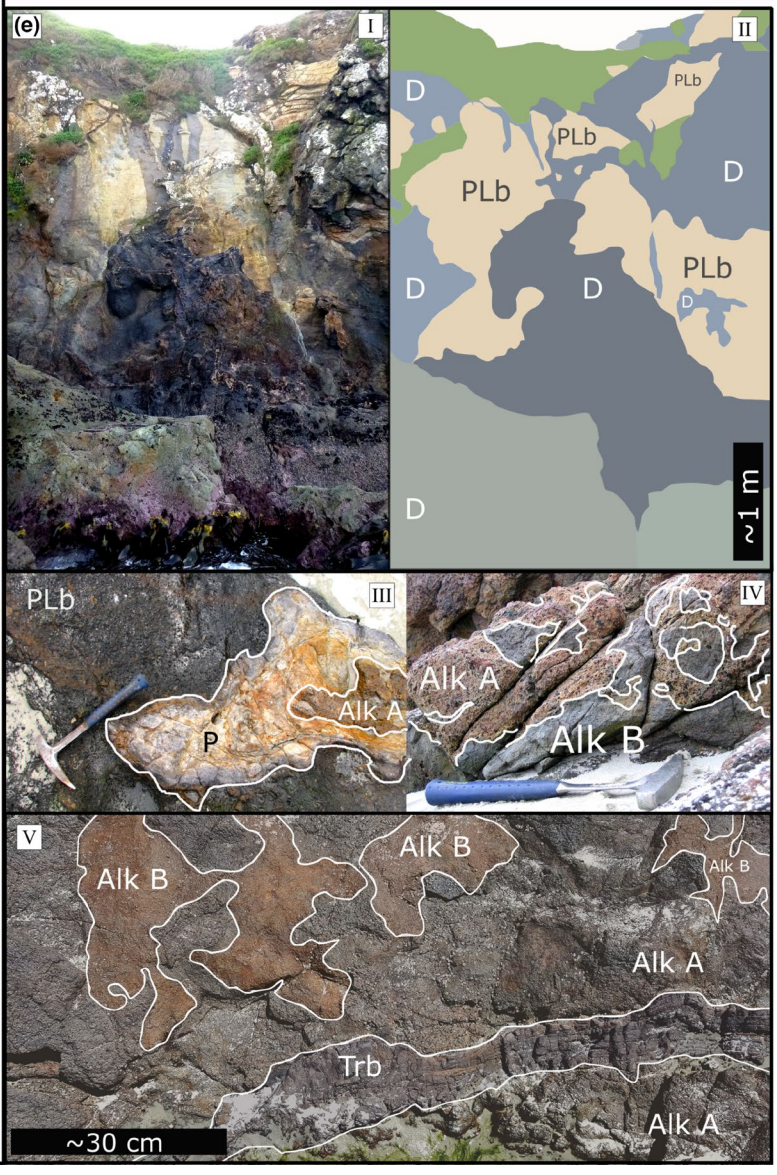
(e)
I
II
D
PLb
PLb
D
PLb
D
D
PLb
D
D
~1 m
PLb
III
P
Alk A
IV
Alk A
Alk B
V
Alk B
Alk B
Alk B
Alk A
Trb
Alk A
~30 cm

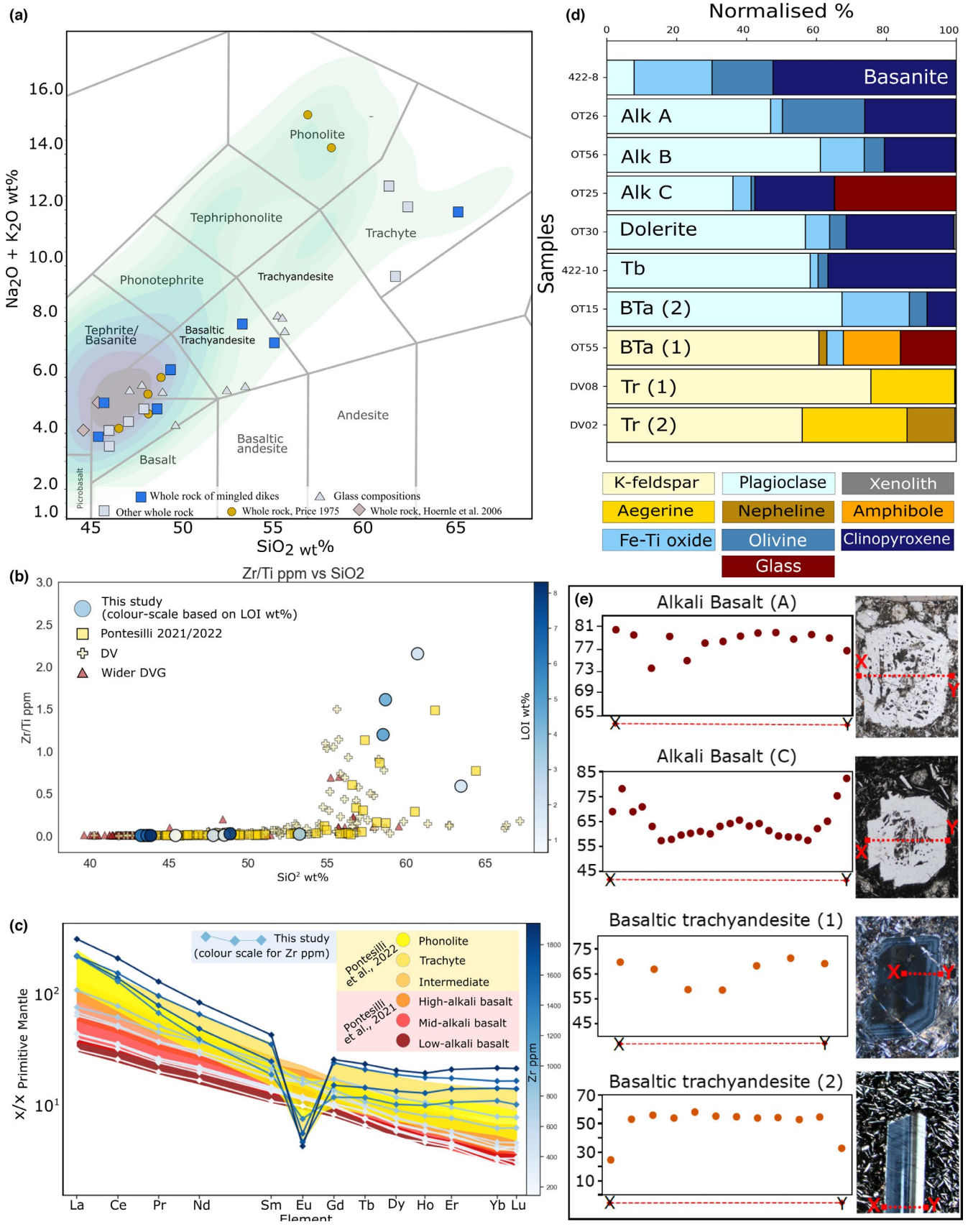

are likely phonolites (e.g. Tr2). Immobile trace element ratios resistant to modification such as Zr/Ti (Pearce & Norry, 1979) display one of these dikes as the most extensively fractionated from the DV, exceeding the range reported from other known DV phonolites (Figure 2b). Crystals from most of the mafic and intermediate dikes display disequilibrium textures and zoning. Crystals analysed from

FIGURE 2 (a) TAS diagram for Otapahi samples; mingled dikes in blue. Other whole-rock = grey boxes; glass = triangles; diamonds = from Hoernle et al., 2006; circles = from Price 1973. Background colour scale indicates the range of compositions reported from the Dunedin Volcano (DV). (b) Spread of samples Zr ppm vs Ti ppm. Blue circles represent whole-rock from this study, with colour scale representing LOI wt%. Yellow boxes = DV compositions reported by Pontesilli et al. (2021 and 2022); plus-box = compilation of DV samples from Scott et al., 2020, triangles = Dunedin volcanic group rocks compiled for Scott et al., 2020. (c) Rare earth element profile for whole-rock samples presented in this study. Normalized to primitive mantle composition (Sun & McDonough, 1989). (d) Modal mineral abundances collected from thinsections from Otapahi, normalized to 100% after secondary minerals (carbonate, unresolvable clay minerals) removed. Labels based on TAS classification. Alk = alkali basalts, tb = trachybasalt. Bta = basaltic trachyandesite, tr = trachyte. All geochemical graphs related with Pypl (Williams et al., 2020) (e) representative mineral profiles of plagioclase crystals from two alkali basalts, and two basaltic trachyandesites (BTa). Complex profiles of Alk C phenocrysts; intensely resorbed phenocrysts in Alk a are less complex. BTa (1), sample modelled as formed by magma mixing, profile shows more variation. Profile (2) normal zoning in BTa (2). Analyses on JEOL JXA-8230 SuperProbe electron probe Microanalyser (EPMA), Victoria University of Wellington, NZ

different dikes display element concentration profiles of varying complexity (Figure 2e), especially within mafic samples.

Magnetic polarity was tested for Subunit A and B of the PLb, alkali basalt, basaltic trachyandesite and a trachyte dikes. All are of normal polarity, narrowing the date, within $^{40}Ar/^{39}Ar$ date error range, to within C5Cn1 (16.26–15.97 Ma) or C5Cn2 (16.40–16.30 Ma; File S1).

4 | DISCUSSION

4.1 | Truly early magma diversity?

Contact with pre-volcanic strata is obscured, but the lack of older igneous lithic fragments in the oldest diatremes, which quarried down to basement schist (Baxter & White, submitted), strongly implies that examined rocks represent the earliest volcanic products. Later-formed diatremes contain igneous lithic fragments derived by fragmentation of concurrently emplaced dikes (Baxter & White, submitted).

At Otapahi, fluidal dike margins and magma mingling forming peperites with the PLb (Martin & White, 2002), indicates dike intruded unconsolidated pumice (Kokelaar, 1982; Skilling et al., 2002). Successive intruding commingling of geochemically diverse dikes hosted within the PLb ranges from centimetre to metre scale (Figure 1d) demonstrates contemporaneous emplacement of multiple magmas; earlier dikes must have still been partially molten for mingling to occur. Dikes have been observed to cool below 500°C 20 years after intrusion, and modelled to cool below 100°C within a century (Connor et al., 1997). This thermally limited timeframe precludes derivation of the different magmas from a single static magma body evolving over 100–1000s of years in the crust (Schmincke, 2007).

Both textures and compositions indicate magmas with different histories, implying injection of multiple batches into the area. Although alteration has affected major element compositions, immobile trace element ratios and REE abundances (Figure 2b; Table 1) demonstrate Otapahi's compositional diversity is equal to the diversity recorded from entire DV's sequence (Figure 2b). Detailed studies on crystals from throughout the DV history indicate persistent magma recharge and mixing events across the entire plumbing system (Pontesilli et al., 2021). Magma mixing processes are inferred for Otapahi from chemical zoning of pumice deposit (Figure S1; Baxter & White, submitted), simple mixing models for intermediate composition dikes (Figure 2a), abundant disequilibrium textures and complex element profiles for mafic and intermediate rock phenocrysts (Figure 2e). Samples enriched in alkalis and trace elements may result from parental magmas generated by smaller degrees of partial melting, wall-rock interactions, longer residence/evolution times, or some combination (Martin et al., 2010; Pontesilli et al., 2022).

4.2 | Simultaneous accumulation, evolution and mobilization

It is well established that more dikes arrest than successfully erupt (Gudmundsson, 2002). These 'failed eruptions' have been argued to precede the formation of continental monogenetic centres (Németh et al., 2003), with Brenna et al., 2011 demonstrating a range of pre-eruptive magma plumbing complexities for monogenetic volcanoes of Jeju Island, Korea. Modern failed eruptions are reported from rift settings, stratovolcanoes, monogenetic fields, and shield volcanoes (Calais et al., 2008; Cervelli et al., 2002). Dike advance can be impeded by regional and local stress regimes, crustal heterogeneities and lithological boundaries (Gudmundsson, 2002; Tibaldi, 2015). We infer accumulation of mafic magmas at the MOHO (Figure 3), and it is unlikely that regional stress regimes or the lithologically monotonous Otago Schist inhibited ascent of these magmas to the DV; in the broader DVG, widely spaced and sporadic eruptions of basaltic magmas began at 24.8 Ma (Hoernle et al., 2006). The regional Otago Schist basement, an exhumed accretionary complex (Mortimer, 2003), structurally complex with many faults, (Carter, 1988) is floored at 10–15 km depth by a regional decollement (Beanland & Berryman, 1989). As middle crust is often a 'leaky transfer zone' (e.g. Putirka, 2017) the middle crust below Dunedin probably initially trapped little, if any, ascending magma. Faults in the shallow crust can arrest dike propagation and/or divert magma to sills or other reservoirs (e.g. Tibaldi, 2015). Discrete pockets of stalled magmas at different crustal levels evolved separately (Figure 3), undergoing varied differentiation processes producing disparate crystal element profiles and geochemical characteristics of Otapahi.

Quantitative modelling of similar crystal zonation elsewhere in the DV places storage sites at depths of 5–14 km depth for evolved

TABLE 1 Major and trace elements from whole-rock analyses

	Samples													
Sample	**OT80-B**	**OT80-C**	**OT26-E**	**OT26-GM**	**OT56**	**OT30**	**OT25**	**422–10**	**OT15**	**OT55**	**DV08**	**422–6**	**OT58**	**DV02**
Rock name	Alkali Basalt					Basalt	Alkali basalt	Trachybasalt	Basaltic trachyandesite		Trachyte			
Reference in text	Alk A	Alk A	Alk A	–	Alk B	Dolerite	Alk C	Trb	Bta (2)	Bta (1)	Tr(1)	–	–	Tr(2)
	Mingled compositions							Mingled compositions						
Major element (wt%)														
Al_2O_3	13.04	12.56	12.8	15.39	17.19	15.3	14.44	16.9	14.95	17.16	15.68	18.58	19.98	17.45
BaO	0.03	0.03	0.03	0.03	0.04	0.03	0.03	0.06	0.06	0.08	0.01	<0.01	0.01	<0.01
CaO	11.25	11.1	11.05	10.75	10.5	10.2	8.18	8.5	5.71	4.26	0.53	0.52	0.65	0.9
Cr_2O_3	0.04	0.08	0.05	0.01	0.01	0.02	0.02	0.01	0.01	<0.01	0.01	<0.01	<0.01	<0.01
Fe_2O_3	11.79	12	11.94	10.2	12.77	11.9	12.62	11.12	11.25	10.17	5.56	4.97	5.13	5.99
K_2O	1.11	0.75	0.92	1.12	1.37	1.36	1.26	1.95	2.78	2.65	4.97	5.15	5.07	5.2
MgO	7.68	9.97	8.82	5.6	4.25	4.99	4.5	3.85	2.06	1.6	0.43	0.47	1.2	0.25
MnO	0.16	0.17	0.17	0.15	0.18	0.17	0.17	0.18	0.17	0.22	0.13	0.14	0.14	0.13
Na_2O	2.57	2.77	2.27	2.78	3.48	3.19	2.95	3.99	3.96	4.37	6.29	6.77	3.75	6.2
P_2O_5	0.42	0.45	0.31	0.39	0.79	0.39	0.44	0.61	0.54	0.63	0.04	0.04	0.04	0.02
SiO_2	43.39	43.72	43.2	43.59	45.4	47.78	43.83	48.48	53.24	48.85	63.46	58.68	58.53	60.71
SrO	0.06	0.06	0.05	0.06	0.09	0.06	0.06	0.08	0.04	0.07	<0.01	<0.01	<0.01	<0.01
TiO_2	2.66	2.45	2.15	2.43	3.34	2.63	2.75	2.24	1.58	1.42	0.2	0.08	0.07	0.09
LOI	5.73	3.17	6.46	6.83	0.64	2.07	8.31	1.64	3.34	7.9	2.01	4.55	4.94	2.24
Total	100.1	101.6	100.45	99.62	100.3	100.3	99.94	99.84	99.86	100.25	99.53	100.15	99.72	99.48
Elements (ppm)														
Ba	288	268	260	297	347	304	297	551	533	675	60.2	39.2	80.2	25.5
Ce	60.1	60.5	44.6	55.4	87.4	61.4	61.5	90	106.5	134.5	265	240	224	361
Cr	300	540	410	130	40	80	90	60	20	<10	<10	<10	<10	<10
Cs	0.54	1.4	2.97	4.62	0.65	0.94	0.74	2.41	3.08	3.17	0.56	10.3	3.16	16.1
Dy	4.22	4.17	3.62	4.31	5.52	4.91	4.81	5.44	8.42	6.43	13.5	9.58	7.29	14.75
Er	2.07	2.04	1.94	2.14	2.7	2.42	2.5	2.71	4.48	3.57	8.16	6.54	4.96	9.79
Eu	1.87	1.95	1.61	1.85	2.59	1.89	1.95	2.61	2.54	2.82	0.91	0.76	1.23	0.7
Ga	19.1	17.7	19.8	23.3	24.1	24.1	23.5	24.7	29.7	25.9	36	40.5	33.2	47.8
Gd	5.62	5.82	4.77	5.63	7.45	5.99	5.99	6.92	9.97	7.92	13.95	8.75	6.84	14.9
Ge	<5	<5	<5	<5	<5	<5	<5	<5	<5	<5	<5	<5	<5	<5
Hf	4.3	4	3.7	4.3	5.3	4.8	4.7	5.5	8.9	7.6	25.8	24.8	16	39.3

TABLE 1 (Continued)

	Samples													
Sample	OT80-B	OT80-C	OT26-E	OT26-GM	OT56	OT30	OT25	422–10	OT15	OT55	DV08	422–6	OT58	DV02
Ho	0.78	0.79	0.74	0.81	1.06	0.95	0.93	1.05	1.69	1.28	2.83	2.05	1.59	3.1
La	29	29.1	21.1	26.5	42.6	29.6	29.4	45.6	50.8	72.3	147	145.5	145	208
Lu	0.22	0.2	0.2	0.24	0.3	0.3	0.28	0.33	0.56	0.45	1.19	1.01	0.73	1.54
Nb	39.3	39.4	28.4	36.4	58.6	38.2	40.5	64.5	52.5	114.5	220	238	156.5	375
Nd	27.5	28.6	22	25.9	40.4	28.6	29.1	38	48.7	50.3	86.7	64.1	51.5	110.5
Pr	6.76	7.06	5.35	6.48	10	7.05	7.09	9.89	12.2	13.9	25.8	21.2	18.1	34.7
Rb	27.8	18.3	22.8	29.4	35.3	40	31.3	46.2	91.8	68.8	196	260	209	371
Sm	5.9	6.01	4.69	5.71	8.38	6.11	6.31	7.51	10.45	9.14	15.2	10.7	8.16	18.5
Sn	2	2	2	2	2	2	2	2	4	4	12	14	10	19
Sr	585	598	513	644	878	560	554	773	412	756	36.9	27.6	68.1	19.8
Ta	2.5	2.5	1.9	2.7	3.9	2.5	2.7	3.9	3.4	6.9	14.1	16.8	14.1	23.6
Tb	0.8	0.79	0.69	0.79	1.04	0.93	0.92	1.02	1.52	1.13	2.2	1.51	1.23	2.46
Th	4.02	3.69	2.87	3.55	5.21	5.08	4.44	6.25	11.1	10.85	39.3	46.1	43.9	61.4
Tm	0.27	0.26	0.23	0.27	0.35	0.3	0.33	0.37	0.62	0.49	1.24	1.03	0.77	1.51
U	1.05	1.03	0.76	0.93	1.44	1.32	1.04	1.67	2.79	2.92	9.77	10.4	9.77	16.05
V	368	284	287	287	305	324	318	173	77	24	<5	<5	<5	<5
W	144	186	206	1 140	540	466	325	314	455	344	392	27	120	208
Y	20.1	20.2	18.4	20.9	26.9	24	23.7	26.9	43.1	33.5	77.3	57.4	44.5	82.6
Yb	1.61	1.54	1.42	1.59	2.07	1.96	1.94	2.23	3.79	2.98	7.89	6.8	5.25	10.35
Zr	175	166	144	174	226	194	193	243	357	384	1 180	1 290	839	1940
As	0.6	0.4	0.5	0.7	0.8	1.5	0.7	1.2	0.9	0.7	0.5	1.9	3.5	7
Bi	0.01	<0.01	0.01	0.02	<0.01	0.01	0.03	0.02	0.03	0.03	0.1	0.36	0.23	0.38
Hg	0.062	0.094	0.108	0.458	0.257	0.295	0.152	0.216	0.317	0.174	0.238	0.01	0.042	0.09
In	0.014	0.022	0.012	0.022	0.02	0.016	0.039	0.02	0.049	0.051	0.097	0.019	0.012	0.022
Re	0.001	0.003	0.002	0.006	0.003	0.004	0.002	0.003	0.004	0.002	0.003	<0.001	0.001	0.002
Sb	<0.05	<0.05	<0.05	<0.05	0.05	0.05	<0.05	0.05	<0.05	<0.05	0.09	0.11	0.1	0.28
Sc	4.1	5	4.8	5.6	3.5	3.2	7.3	2.8	2.9	2.8	1.1	0.6	0.4	0.5
Se	0.7	1	0.3	0.4	1	0.4	0.6	0.9	0.8	0.7	1.1	0.6	0.6	1
Te	0.02	0.02	0.01	0.01	0.01	0.01	0.02	0.02	0.02	0.01	0.01	0.01	0.01	0.01
Tl	0.04	0.05	0.15	0.26	0.1	0.09	0.23	0.08	0.13	0.1	0.09	0.12	0.2	0.78
Ag	<0.5	<0.5	<0.5	<0.5	<0.5	<0.5	<0.5	<0.5	<0.5	<0.5	<0.5	<0.5	<0.5	<0.5

(Continues)

TABLE 1 (Continued)

Sample	Samples														
	OT80-B	OT80-C	OT26-E	OT26-GM	OT56	OT30	OT25	422–10	OT15	OT55	DV08	422–6	OT58	DV02
Cd	0.7	0.6	<0.5	0.5	<0.5	<0.5	0.7	<0.5	<0.5	<0.5	0.5	<0.5	<0.5	<0.5
Co	64	76	78	178	102	100	74	67	76	57	52	5	16	25
Cu	33	36	43	49	32	40	41	39	15	17	9	7	5	12
Li	10	10	10	10	10	10	10	10	20	20	30	50	20	80
Mo	2	2	2	2	3	2	1	3	2	2	2	5	5	4
Ni	133	220	181	94	25	40	34	34	7	5	2	12	5	1
Pb	<2	3	6	3	<2	5	4	5	11	2	32	21	19	33
Sc	25	26	25	16	16	24	19	13	14	2	1	<1	<1	<1
Zn	105	99	105	102	111	109	71	107	141	116	165	143	149	222

magmas, 16–29 km for intermediate compositions (Pontesilli et al., 2022), 19–30 km for high-alkali basalts which bypass the shallow plumbing system, while low-alkali km basalts undergo polybaric crystallization from the lithospheric mantle to upper crustal levels of the plumbing system (Pontesilli et al., 2021). Their quantitative modelling of the broader volcano's plumbing system concurs with our qualitative inferences about the plumbing established beneath Otapahi, where similar diversity shows that the complex system was established and emplacing both alkaline, subalkaline, primitive and evolved rocks during the earliest stages of volcanism.

Within intraplate volcanic fields, larger, complex volcanoes are suggested to develop above loci of peak mantle productivity (Schmincke, 2007). Here, we suggest their compositional diversity may first develop due to multiple failed eruptions that build a substantial subterranean magmatic system prior to surficial volcanic activity. This pattern mimics at smaller temporal and spatial scales that of large long-lived continental arcs, where similar subterranean system-building and evolution can precede main eruptive periods (Annen et al., 2006). Unlike central volcanoes of continental arcs, here there was a great diversity of compositions in a group of magmas that erupted nearly synchronously to produce some of the earliest rocks known from the volcano (published Ar–Ar; see compilation Scott et al., 2020). These compositions cover the range erupted over the remainder of the volcano's activity, implying that these early and diverse magmas and storage zones represent the template for the volcano's long-term plumbing.

Eruption of phonolite magma to form the PLb disrupted and destabilized a maturing magmatic system that comprised multiple, primitive-to-evolved, storage zones tiered through the crust. Incomplete mixing drove transition of the PLb from phenocryst-poor phonolite glass at the base to one with mafic phenocrysts like those in alkali basalt dikes, carried in evolved glassy pyroclasts. The basalt-triggered eruption from this shallow storage zone seems to have caused mobilization and coalescence of deeper magmas (Marzoli et al., 2015), perhaps by initiating a downward-propagating decompression wave, as was suggested to explain deepening seismicity before eruption at Eyjafjallajökull in 2010 (Tarasewicz et al., 2012).

Models in which a volcano commences activity by erupting primitive material (Khalaf et al., 2018; Sato et al., 1990), or with emplacement of evolved lavas (Pánisová et al., 2018; Panter et al., 1997), are not appropriate for the DV. Petrography and geochemistry of compositionally diverse rocks emplaced penecontemporanously at Otapahi indicate a magmatic system that had already matured before the volcano's oldest-dated rock was emplaced.

4.3 | Precedent set for further activity

DV marks a locus of higher mantle productivity within the low-output DVG (McLeod & White, 2018; Scott et al., 2020). Multiple failed eruptions, probably controlled by structural features of the upper crust, developed a complex magmatic system above this locus. Subsequent divergence of evolution developed a diverse suite of early magmas, some highly evolved. Eruptions were triggered by

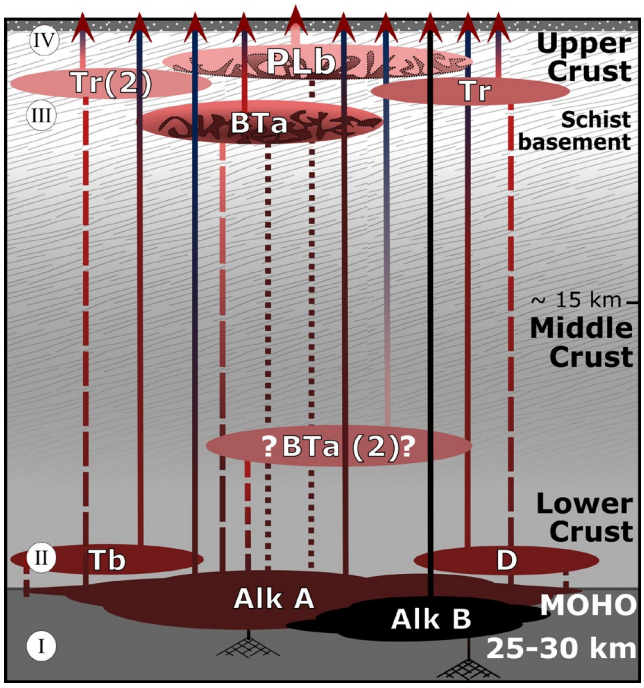

FIGURE 3 Top stippled layer = Cenozoic sedimentary sequence. (I) Accumulation of Alk a and Alk B near MOHO, favoured by mechanical boundary between mantle and lower crust. (II) Magma batches ascend into lower crust after different degrees of fractionation. Some magmas mix. (III) Magmas ascending through the crust (dashed lines) are trapped by structural discontinuities, then continue evolving. Some mix with mafic magmas (dotted lines). IV). Magmas developed across the entire system were mobilized and emplaced (solid lines) after the PLb-forming eruption. This produced the diverse array of rocks emplaced quickly at Otapahi during the initiation of the Dunedin Volcano. Alk, alkali basalt; BTa, basaltic trachyandesite; D, dolerite; PLb, pumice lapilli beds; tb, trachybasalt; tr, trachyte

mixing/recharge events that destabilized the system, leading to the mobilization, eruption and intrusion of multiple magmas at Otapahi.

Above this zone of increased mantle productivity, magma supplied more persistently and at higher rates than elsewhere in the DVG continued this pattern over 5 Myr, with differentiation at various levels in the crust (Pontesilli et al., 2021, 2022). Repeated eruption of the same suite of compositionally diverse magmas characterizes DV's history (Coombs et al., 2008). It implies the persistent presence, or repeated production, of multiple, unintegrated, magma bodies beneath the long-lived DV. Repeated eruptions of the same range of magmas suggest a system of tiered reservoirs (Maclennan, 2019) failing to fully integrate through millions of years of slow volcano growth, never developing the vertical connectivity of a transcrustal magma system (Cashman et al., 2017). The Otapahi succession set the pattern for the volcano's overall evolution.

5 | CONCLUSIONS

DV's earliest dated volcanic rocks display a remarkable compositional range, and include mingled igneous rocks from different magmas, emplaced pene-contemporaneously at Otapahi at different points in their compositional evolutions. Their rapid, successive emplacement implies a complex magmatic system that had previously formed in the crust. The formation of the magmatic system involved multiple failed eruptions that delivered magma to different levels in the crust, where it underwent various differentiation processes over different periods of time. This same behaviour, represented at Otapahi, appears to have subsequently continued over millions of years, over which the volcano continued to produce a similar range of magma compositions. At this low-flux intraplate continental volcano, a complex weakly interconnected magma system developed very early, exhibiting a style of activity that persisted for another 5 million years.

ACKNOWLEDGEMENTS

Access to Otapahi was made possible by the Yellow-eyed Penguin Trust and the Neil family. Funding was provided to RJMB by U. Otago MSc scholarship and NZ Federation of Graduate Women.

CONFLICT OF INTEREST

The authors have no conflicts of interest to declare in relation to this work.

DATA AVAILABILITY STATEMENT

The data that supports the findings of this study are available in the supplementary material of this article.

ORCID

Rachael J. M. Baxter https://orcid.org/0000-0003-4177-5630

REFERENCES

Annen, C., Blundy, J. D., & Sparks, R. S. J. (2006). The genesis of intermediate and silicic magmas in deep crustal hot zones. *Journal of Petrology*, *47*, 505–539. https://doi.org/10.1093/petrology/egi084

Baxter, R. J. M., White, J. D. L. (submitted), Complex arrangement of early disparate pyroclastic and intrusive rock heralded onset of intraplate Dunedin Volcano

Beanland, S., & Berryman, K. R. (1989). Style and episodicity of late quaternary activity on the Pisa-Grandview fault zone, Central Otago, New Zealand. *New Zealand Journal of Geology and Geophysics*, *32*, 451–461. https://doi.org/10.1080/00288306.1989.10427553

Benson, W.N., 1968, Dunedin District. New Zealand Geological Survey miscellaneous series map, scale 1:50,000:

Brenna, M., Cronin, S. J., Németh, K., Smith, I. E. M., & Sohn, Y. K. (2011). The influence of magma plumbing complexity on monogenetic eruptions, Jeju Island, Korea. *Terra Nova*, *23*, 70–75. https://doi.org/10.1111/j.1365-3121.2010.00985.x

Brenna, M., Cronin, S. J., Smith, I. E. M., Sohn, Y. K., & Maas, R. (2012). Spatio-temporal evolution of a dispersed magmatic system and its implications for volcano growth, Jeju Island Volcanic Field, Korea. *Lithos*, *148*, 337–352. https://doi.org/10.1016/j.lithos.2012.06.021

Calais, E., d'Oreye, N., Albaric, J., Deschamps, A., Delvaux, D., Déverchère, J., Ebinger, C., Ferdinand, R. W., Kervyn, F., Macheyeki, A. S., Oyen, A., Perrot, J., Saria, E., Smets, B., Stamps, D. S., & Wauthier, C. (2008). Strain accommodation by slow slip and dyking in a youthful continental rift, East Africa. *Nature*, *456*, 783–788. https://doi.org/10.1038/nature07478

Carter, R. M. (1988). Post-breakup stratigraphy of the kaikoura synthem (cretaceous-cenozoic), continental margin, southeastern New Zealand. *New Zealand Journal of Geology and Geophysics*, *31*, 405–429. https://doi.org/10.1080/00288306.1988.10422141

Cashman, K. V., Sparks, R. S. J., & Blundy, J. D. (2017). Vertically extensive and unstable magmatic systems: A unified view of igneous processes. *Science*, *355*, doi:10.1126/science.aag3055.

Cervelli, P., Segall, P., Amelung, F., Garbeil, H., Meertens, C., Owen, S., Miklius, A., & Lisowski, M. (2002). The September 12, 1999 Upper East Rift Zone dike intrusion at Kilauea Volcano, Hawaii. *Journal of Geophysical Research Solid Earth*, *107*, ECV 3-1–ECV 3-13. https://doi.org/10.1029/2001JB000602

Chevrel, M. O., Guilbaud, M. N., & Siebe, C. (2016). The ~AD 1250 effusive eruption of El metate shield volcano (Michoacán, Mexico): Magma source, crustal storage, eruptive dynamics, and lava rheology. *Bulletin of Volcanology*, *78*, 1–28. https://doi.org/10.1007/s00445-016-1020-9

Coombs, D S., & Reay, A. (1986). *Excursion C2: Cenozoic alkalic and tholeitic volcanism eastern south island*. University of Otago.

Connor, C. B., Conway, F. M., & Sigurdsson, H. (2000). Basaltic volcanic fields. In *Encyclopedia of volcanoes* (pp. 331–343). Academic Press.

Connor, C. B., Lichtner, P. C., Conway, F. M., Hill, B. E., Ovsyannikov, A. A., Federchenko, I., Doubik, Y., Shapar, V. N., & Taran, Y. A. (1997). Cooling of an igneous dike 20 yr after intrusion. *Geology*, *25*, 711–714. https://doi.org/10.1130/0091-7613(1997)025<0711:COAIDY>2.3.CO;2

Coombs, D. S., Adams, C. J., Roser, B. P., & Reay, A. (2008). Geochronology and geochemistry of the Dunedin volcanic group, eastern Otago, New Zealand. *New Zealand Journal of Geology and Geophysics*, *51*, 195–218. https://doi.org/10.1080/00288300809509860

Duda, A., & Schmincke, H. U. (1985). Polybaric differentiation of alkali basaltic magmas: Evidence from green-core clinopyroxenes (Eifel, Frg). *Contributions to Mineralogy and Petrology*, *91*, 340–353. https://doi.org/10.1007/BF00374690

Finn, C. A., Müller, R. D., & Panter, K. S. (2005). A Cenozoic diffuse alkaline magmatic province (DAMP) in the Southwest Pacific without rift or plume origin. *Geochemistry, Geophysics, Geosystems*, *6*, 1–26. https://doi.org/10.1029/2004GC000723

Gudmundsson, A. (2002). Emplacement and arrest of sheets and dykes in central volcanoes. *Journal of Volcanology and Geothermal Research*, *116*, 279–298. https://doi.org/10.1016/S0377-0273(02)00226-3

Hoernle, K., White, J. D. L., van den Bogaard, P., Hauff, F., Coombs, D. S., Werner, R., Timm, C., Garbe-Schönberg, D., Reay, A., & Cooper, A. F. (2006). Cenozoic intraplate volcanism on New Zealand: Upwelling induced by lithospheric removal. *Earth and Planetary Science Letters*, *248*, 335–352. https://doi.org/10.1016/j.epsl.2006.06.001

Jankovics, M. É., Harangi, S., Németh, K., Kiss, B., & Ntaflos, T. (2015). A complex magmatic system beneath the Kissomlyó monogenetic volcano (western Pannonian Basin): Evidence from mineral textures, zoning and chemistry. *Journal of Volcanology and Geothermal Research*, *301*, 38–55. https://doi.org/10.1016/j.jvolgeores.2015.04.010

Khalaf, E. E. D. A. H., Sano, T., & Tsutsumi, Y. (2018). Evolution of monogenetic rift-related alkaline magmatism in South Egypt: Insight from stratigraphy, geochronology, and geochemistry of the Natash volcanics. *Journal of African Earth Sciences*, *147*, 450–476. https://doi.org/10.1016/j.jafrearsci.2018.05.024

Klügel, A., Hoernle, K. A., Schmincke, H., & White, J. D. L. (2000). The chemically zoned 1949 eruption on La Palma (Canary Islands): Petrologic evolution and magma supply dynamics of. *Journal of Geophysical Research*, *105*, 5997–6016.

Kokelaar, B. P. (1982). Fluidization of wet sediments during the emplacement and cooling of various igneous bodies. *Journal of the Geological Society*, *139*, 21–33. https://doi.org/10.1144/gsjgs.139.1.0021

Maclennan, J. (2019). Mafic tiers and transient mushes: Evidence from Iceland. *Philosophical Transactions of the Royal Society A*, *377*, 20180021. https://doi.org/10.1098/rsta.2018.0021

Martin, A. P., Cooper, A. F., & Dunlap, W. J. (2010). Geochronology of mount morning, Antarctica: Two-phase evolution of a long-lived trachyte-basanite-phonolite eruptive center. *Bulletin of Volcanology*, *72*, 357–371. https://doi.org/10.1007/s00445-009-0319-1

Martin, U., & White, J. D. L. (2001). Depositional and eruptive mechanisms of density current deposits from a submarine vent at the Otago peninsula. *New Zealand: Special Publication – International Association of Sedimentologists*, *31*, 245–260.

Martin, U., & White, J. D. L. (2002). Melting and mingling of phonolitic pumice deposits with intruding dykes: An example from the Otago peninsula. *New Zealand: Journal of Volcanology and Geothermal Research*, *114*, 129–146. https://doi.org/10.1016/S0377-0273(01)00286-4

Marzoli, A., Aka, F. T., Merle, R., Callegaro, S., & N'ni, J. (2015). Deep to shallow crustal differentiation of within-plate alkaline magmatism at Mt. Bambouto volcano, Cameroon Line. *Lithos*, *220-223*, 272–288. https://doi.org/10.1016/j.lithos.2015.02.005

McLeod, O. E., & White, J. D. L. (2018). Petrogenetic links between the Dunedin Volcano and peripheral volcanics of the Karitane suite. *New Zealand Journal of Geology and Geophysics*, *61*, 543–561. https://doi.org/10.1080/00288306.2018.1518248

Mortimer, N. (2003). A provisional structural thickness map of the Otago Schist, New Zealand. *American Journal of Science*, *303*, 603–621. https://doi.org/10.2475/ajs.303.7.603

Németh, K., White, J. D. L., Reay, A., & Martin, U. (2003). Compositional variation during monogenetic volcano growth and its implications for magma supply to continental volcanic fields. *Journal of the Geological Society*, *160*, 523–530. https://doi.org/10.1144/0016-764902-131

Pánisová, J., Balázs, A., Zalai, Z., Bielik, M., Horváth, F., Harangi, S., Schmidt, S., & Götze, H. J. (2018). Intraplate volcanism in the Danube Basin of NW Hungary: 3D geophysical modelling of the late Miocene Pásztori volcano. *International Journal of Earth Sciences*, *107*, 1713–1730. https://doi.org/10.1007/s00531-017-1567-5

Panter, K. S., Kyle, P. R., & Smellie, J. L. (1997). Petrogenesis of a phonolite-trachyte succession at mount sidley, marie byrd land, Antarctica. *Journal of Petrology*, *38*, 1225–1253. https://doi.org/10.1093/petroj/38.9.1225

Pearce, J. A., & Norry, M. J. (1979). Petrogenetic implications of Ti, Zr, Y, and Nb variations in volcanic rocks. *Contributions to Mineralogy and Petrology*, *69*, 33–47. https://doi.org/10.1007/BF00375192

Pontesilli, A., Brenna, M., Mollo, S., Masotta, M., Nazzari, M., Le Roux, P., & Scarlato, P. (2022). Trachyte-phonolite transition at Dunedin Volcano: Fingerprints of magma plumbing system maturity and mush evolution. *Lithos*, *408–409*, 106545. https://doi.org/10.1016/j.lithos.2021.106545

Pontesilli, A., Brenna, M., Ubide, T., Mollo, S., Masotta, M., Caulfield, J., Le Roux, P., Nazzari, M., Scott, J. M., & Scarlato, P. (2021). Intraplate basalt alkalinity modulated by a lithospheric mantle filter at the Dunedin Volcano (New Zealand). *Journal of Petrology*, *62*, 1–36. https://doi.org/10.1093/petrology/egab062

Putirka, K. D. (2017). Down the crater: Where magmas are stored and why they erupt. *Elements*, *13*, 11–16. https://doi.org/10.2113/gselements.13.1.11

Reilly, W. I. (1972). New Zealand journal of geology and geophysics Gravitational expression of the Dunedin Volcano. *New Zealand Journal of Geology and Geophysics*, *15*, 16–21. https://doi.org/10.1080/00288306.1972.10423943

Sato, H., Aramaki, S., Kusakabe, M., Hlrabayashi, J. I., Sano, Y., Nojiri, Y., & Tchoua, F. (1990). Geochemical difference of basalts between polygenetic and monogenetic volcanoes in the central part of the Cameroon volcanic line. *Geochemical Journal*, *24*, 357–370. https://doi.org/10.2343/geochemj.24.357

Schmincke, H. U. (2007). The quaternary volcanic fields of the east and west Eifel (Germany). In *Mantle plumes* (pp. 241–322). Springer.

Scott, J. M., Pontesilli, A., Brenna, M., White, J. D. L., Giacalone, E., Palin, J. M., & le Roux, P. J. (2020). The Dunedin volcanic group and a

revised model for Zealandia's alkaline intraplate volcanism the Dunedin volcanic group and a revised model for Zealandia's alkaline. *New Zealand Journal of Geology and Geophysics*, *0*, 1–20. https://doi.org/10.1080/00288306.2019.1707695

Skilling, I. P., White, J. D. L., & McPhie, J. (2002). Peperite: A review of magma-sediment mingling. *Journal of Volcanology and Geothermal Research*, *114*, 1–17. https://doi.org/10.1016/S0377-0273(01)00278-5

Sun, S. S., & McDonough, W. F. (1989). Chemical and isotopic systematics of oceanic basalts: Implications for mantle composition and processes. *Geological Society Special Publication*, *42*, 313–345. https://doi.org/10.1144/GSL.SP.1989.042.01.19

Tarasewicz, J., White, R. S., Woods, A. W., Brandsdóttir, B., & Gudmundsson, M. T. (2012). Magma mobilization by downward-propagating decompression of the Eyjafjallajökull volcanic plumbing system. *Geophysical Research Letters*, *39*, 1–5. https://doi.org/10.1029/2012GL053518

Tibaldi, A. (2015). Structure of volcano plumbing systems: A review of multiparametric effects. *Journal of Volcanology and Geothermal Research*, *298*, 85–135. https://doi.org/10.1016/j.jvolgeores.2015.03.023

Williams, M., Schoneveld, L., Mao, Y., Klump, J., Gosses, J., Dalton, H., Bath, A., & Barnes, S. (2020). Pyrolite: Python for geochemistry. *Journal of Open Source Software*, *5*, 2314. https://doi.org/10.21105/joss.02314

Wood, C. A. (1979). Monogenetic volcanoes of the terrestrial planets. In *Proceedings of Lunar Planet Science Conference 10th, Houston, Tex., March 19-23, 1979* (pp. 2815–2840). Elsevier Science B.V.

SUPPORTING INFORMATION

Additional supporting information may be found in the online version of the article at the publisher's website.

Supporting Information S1 Methods used
Supporting Information S2 Supplementary figures
Supporting Information S3 Results

How to cite this article: Baxter, R. J., White, J. D., Brenna, M., & Ohneiser, C. (2022). Pre-eruption magma staging at the long-lived intraplate Dunedin Volcano, New Zealand. *Terra Nova*, 00, 1–11. https://doi.org/10.1111/ter.12585